SINR Analysis of Multi-Waveform STAP

Shannon D. Blunt, Justin Metcalf, and John Jakabosky
Electrical Engineering & Computer Science Dept.
University of Kansas
Lawrence, KS, USA

Braham Himed
Sensors Directorate
Air Force Research Laboratory
Wright-Patterson AFB, Dayton, OH, USA

***Abstract*— A multi-waveform version of space-time adaptive processing denoted as MuW-STAP (or simply μ-STAP) was recently developed that incorporates the training data generated by secondary waveform/filter pairs into the estimation of the sample covariance matrix. This additional training data was found to improve robustness to heterogeneous clutter. Here SINR analysis is used to evaluate the μ-STAP approach under various clutter conditions and with multiple additional sets of training data obtained through the use of multiple different pulse compression filters applied to the same received data.**

Keywords—GMTI, STAP, MIMO

I. INTRODUCTION

In [1] a specific form of multiple-input multiple-output (MIMO) radar was proposed for application to airborne/space-based ground moving target indication (GMTI) in which platform motion necessitates space-time adaptive processing (STAP) for effective clutter cancellation. In general, STAP operates by estimating the covariance matrix of the clutter associated with a given cell-under-test (CUT) for subsequent adaptive filtering to determine if a target is present [2]. Estimation of the covariance matrix is obtained through the use of training data that is near the CUT in range and for which the space-time characteristics are presumed to be homogeneous with that of the CUT. However, due to complicating factors such as clutter non-stationarity, internal clutter motion, contamination of training data, and limited sample support, accurate estimation of the clutter covariance matrix remains a rather difficult task [3,4].

The purpose of the multi-waveform STAP (MuW-STAP or simply μ-STAP) approach proposed in [1] was to facilitate a practical implementation of MIMO for the GMTI application to improvement clutter cancellation. As a brief summary, the goal was to realize a MIMO framework that 1) minimized loss of mainbeam power, 2) employed physically-realizable waveforms that are continuous, relatively bandlimited, and remain constant amplitude, 3) does not assume waveforms are orthogonal, and 4) does not ignore non-ideal array calibration effects. On receive, this practical enhancement was achieved by exploiting the use of secondary waveform/filter pairs as a source of additional training data for covariance estimation.

One of the interesting outcomes of the work in [1] was the observation that a receive-only MIMO mode (thus actually a SIMO mode) could provide much the same performance benefit as the MIMO mode that involved simultaneous emission of more than one waveform. As such, the SIMO instantiation could be implemented on existing systems without modification to the transmit architecture and only the addition of secondary pulse compression channels in parallel. Here we examine this SIMO realization of μ-STAP via SINR analysis under various clutter scenarios, varying number of secondary pulse compression channels, and by varying the swath width from which training data is obtained.

II. MULTI-WAVEFORM STAP

Consider an airborne/space-based GMTI system in which a uniform linear array comprised of N antenna elements transmits M pulses modulated with waveform $s_{\text{prime}}(t)$ in some direction θ_{prime} with respect to antenna boresight. This waveform is designed according to the usual criteria of low range sidelobes and perhaps Doppler tolerance. The standard STAP architecture involves the collection of the resulting echoes over this coherent processing interval (CPI) to perform adaptive processing and subsequently attempt to discern moving targets.

The MIMO instantiation of μ-STAP developed in [1] adds to this standard emission a set of secondary waveforms $s_{\text{sec},k}(t)$ for $k = 1,\cdots$, the purpose of which is to collect additional information about the clutter outside of direction θ_{prime}. These waveforms are designed to have a low cross-correlation with the primary waveform (and each other to a lesser degree) and their emission should possess a spatial beampattern that is markedly lower than the primary emission beampattern in direction θ_{prime} (preferably a null). However, here we shall focus on the SIMO instantiation in which these secondary waveforms are not emitted, yet the μ-STAP receive processing is still performed as if they actually had been.

For this SIMO framework, the received signal is the same as for standard STAP which, for the m^{th} pulse and the n^{th} antenna element is

$$y(m,n,t) = s_{\text{prime}}(t) * x_{\text{prime}}(t) + v(t)\,, \qquad (1)$$

where $x_{\text{prime}}(t)$ comprises the echoes from the primary waveform, the operation $*$ represents convolution, and $v(t)$ is additive noise. The μ-STAP approach [1] then pulse compresses this received signal according to each of the K+1 waveforms as

This work was supported by a subcontract with Booz, Allen and Hamilton for research sponsored by the Air Force Research Laboratory (AFRL) under Contract FA8650-11-D-1011.

$$
\begin{aligned}
z_{\text{prime}}(m,n,t) &= h_{\text{prime}}(t) * y(m,n,t) \\
z_{\text{sec},1}(m,n,t) &= h_{\text{sec},1}(t) * y(m,n,t) \\
&\vdots \\
z_{\text{sec},K}(m,n,t) &= h_{\text{sec},K}(t) * y(m,n,t)
\end{aligned} \tag{2}
$$

where $h_{\text{prime}}(t)$ is the pulse compression filter corresponding to the primary waveform and $h_{\text{sec},k}(t)$ is the pulse compression filter corresponding to the k^{th} secondary waveform. These pulse compression filters may be matched filters or some form of mismatch filters. The multiple waveform-dependent receive channels in (2) can clearly be obtained regardless of whether the K secondary waveforms were transmitted or not.

For look direction θ_{prime} the spatial steering vector $\mathbf{c}_{\text{s}}(\theta_{\text{prime}})$ is formed. Likewise a temporal steering vector $\mathbf{c}_{\text{t}}(\omega_{\text{Dop}})$ is formed for each Doppler frequency ω_{Dop} corresponding to radial motion with respect to the radar. Thus the space-time steering vector is

$$
\mathbf{c}_{\text{st}}(\theta_{\text{prime}}, \omega_{\text{Dop}}) = \mathbf{c}_{\text{t}}(\omega_{\text{Dop}}) \otimes \mathbf{c}_{\text{s}}(\theta_{\text{prime}}) \tag{3}
$$

where $\otimes$ is the Kronecker product. The pulse compressed outputs from (2) are organized in the same manner as the space-time steering vector to yield sets of length-NM space-time snapshots denoted as $\mathbf{z}_{\text{prime}}(t)$ for the primary waveform/filter and $\mathbf{z}_{\text{sec},k}(t)$ for $k = 1,\ldots, K$ for each of the secondary filters. Sampling in fast-time t results in the range cell (delay) index ℓ.

For standard STAP, estimation of the covariance matrix $\mathbf{R}(\ell$ corresponding to the cell-under-test (CUT) involves the "range-focused" (primary) snapshots as

$$
\begin{aligned}
\mathbf{R}(\ell \quad & \left[\mathbf{z}_{\text{prime}}(t)\, \mathbf{z}_{\text{prime}}^{H}(t)\right] \\
& \approx \frac{1}{n(L)} \sum_{\ell \ \ell} \mathbf{z}_{\text{prime}}(\ell \qquad \ell
\end{aligned} \tag{4}
$$

where $(\bullet)^{H}$ signifies complex conjugate transpose, $E[\bullet]$ denotes expectation, $n(L)$ is the number of snapshots in the set L, and ℓ to avoid nulling a possible target. In (4) the expectation is approximated by averaging over the training data surrounding the CUT in range, with guard cells and non-homogeneity detection to excise outliers as necessary (e.g. [3-6]). The resulting sample covariance matrix (SCM) is then used to form the standard STAP filter as

$$
\mathbf{w}(\ell \qquad \ell \qquad) \tag{5}
$$

for application to the CUT snapshot as

$$
\alpha(\ell \qquad \ell \qquad \ell \quad . \tag{6}
$$

The resulting value $\alpha(\ell$ is then compared to a threshold (e.g. generated via CFAR detector) to ascertain the presence of a target.

Using the additional training data channels of (2), μ-STAP can estimate the SCM is two different ways. A new SCM can be defined by supplementing (4) as

$$
\mathbf{R}_{\mu}(\ell \qquad \left[\mathbf{z}_{\text{prime}}(t)\, \mathbf{z}_{\text{prime}}^{H}(t)\right] + \sum_{k=1}^{K} E\left[\mathbf{z}_{\text{sec},k}(t)\, \mathbf{z}_{\text{sec},k}^{H}(t)\right] \tag{7}
$$

where the primary portion is performed in the same manner as in (4). Alternatively, one could use the secondary data without the primary training data to estimate the SCM as

$$
\mathbf{R}_{\mu,\text{NP}}(\ell \qquad \sum_{k=1}^{K} E\left[\mathbf{z}_{\text{sec},k}(t)\, \mathbf{z}_{\text{sec},k}^{H}(t)\right], \tag{8}
$$

where the subscript 'NP' indicates no primary data is used. Thus (8) is the new component of (7) and is estimated as

$$
\mathbf{R}_{\mu,\text{NP}}(\ell \qquad \ell \qquad \ell \ , \tag{9}
$$

where, unlike for the primary training data, the set L_{sec} can include the CUT and guard cells because the secondary channels can be viewed as "unfocused" in range. Following the determination of the modified SCM from (7) or (8), it can be substituted into (5) for subsequent application to the CUT snapshot as in (6).

It is interesting to note that the SIMO μ-STAP approach bears some similarity to the notion of a de-emphasis factor as described in [7,8] in so far as the unfocused secondary data provides much less signal gain on any single range cell such that targets in the secondary training data produce little self-cancellation degradation. Likewise, the SIMO μ-STAP approach can also be viewed as related to multi-resolution STAP approaches such as those in [9,10] that leverage high-resolution SAR imaging to provide GMTI training data (though, per Fig. 1, μ-STAP actually employs lower resolution training data resulting from the smeared cross correlation of the primary waveform and the secondary filters).

III. SINR Analysis

We consider a primary waveform and up to four secondary polyphase-coded FM (PCFM) waveforms generated by the continuous phase modulation (CPM) implementation described in [11-13]. These waveforms are continuous, have constant amplitude, and possess good spectral containment making them feasible as practical radar emissions. The primary is the optimized waveform defined as "performance diversity" in [13] while the four secondary waveforms comprise (k = 1) a waveform designed to have low cross-correlation with the

primary, (k = 2) the time-reversed complex-conjugate of the primary, (k = 3) the time-reversed complex-conjugate of waveform k = 1, and (k = 4) a PCFM-implemented LFM waveform. Based on 3 dB bandwidth, all five waveforms have an approximate time-bandwidth product of 64. Figure 1 illustrates the response of the primary waveform to pulse compression according to the matched filter associated with each of the K+1waveforms as in (2). The unfocused response generated by the cross-correlation smearing is evident. Further, the specific cross-correlation responses also provide diverse modulations of the clutter in range which is shown to enhance SCM estimation.

From the five different channels of pulse compression filtered output via (2) there are numerous combinations that can be formed to estimate the SCM. Denoting 'P' as the primary channel and 'S1' through 'S4' as the four secondary channels, we shall show nine SINR performance curves for each scenario as indicated in Table 1. While these plots are rather busy, the point is to illustrate the impact of incorporating each additional channel of training data.

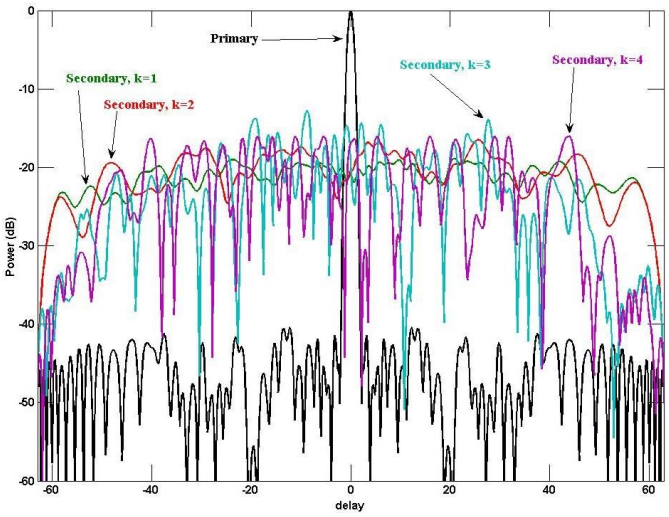

Fig. 1. Matched filter responses to the primary waveform

TABLE I. COMBINATIONS OF TRAINING DATA FOR SINR ANALYSIS

Training data used	Line style/color
P	solid blue
P, S1	solid green
P, S1-S2	solid red
P, S1-S3	solid teal
P, S1-S4	solid purple
S1	dashed green
S1-S2	dashed red
S1-S3	dashed teal
S1-S4	dashed purple

From [14] we shall use the SNR-normalized SINR metric that can be written as

$$\frac{\text{SINR}}{\text{SNR}} = \frac{\sigma_v^2 \left| \mathbf{c}_{\text{st}}^H(\theta,\omega)\hat{\mathbf{R}}^{-1}\mathbf{c}_{\text{st}}(\theta,\omega)\right|^2}{(NM)\,\mathbf{c}_{\text{st}}^H(\theta,\omega)\hat{\mathbf{R}}^{-1}\mathbf{R}_{\text{o}}\hat{\mathbf{R}}^{-1}\mathbf{c}_{\text{st}}(\theta,\omega)}, \tag{10}$$

where σ_v^2 is the noise power, $\mathbf{R}_{\text{o}}$ is the true clutter covariance for the CUT, and $\hat{\mathbf{R}}$ is the estimated SCM using some combination of training data from Table 1. From (10) the (SNR-normalized) optimal SINR is

$$\frac{\text{SINR}_{\text{o}}}{\text{SNR}} = \frac{\sigma_v^2}{NM}\,\mathbf{c}_{\text{st}}^H(\theta,\omega)\mathbf{R}_{\text{o}}^{-1}\mathbf{c}_{\text{st}}(\theta,\omega), \tag{11}$$

which is obtained when $\hat{\mathbf{R}} = \mathbf{R}_{\text{o}}$. The ratio of (10) and (11) then provides the SINR_{o} normalized result

$$\frac{\text{SINR}}{\text{SINR}_{\text{o}}} = \frac{\left|\mathbf{c}_{\text{st}}^H(\theta,\omega)\hat{\mathbf{R}}^{-1}\mathbf{c}_{\text{st}}(\theta,\omega)\right|^2}{\left(\mathbf{c}_{\text{st}}^H(\theta,\omega)\hat{\mathbf{R}}^{-1}\mathbf{R}_{\text{o}}\hat{\mathbf{R}}^{-1}\mathbf{c}_{\text{st}}(\theta,\omega)\right)\left(\mathbf{c}_{\text{st}}^H(\theta,\omega)\mathbf{R}_{\text{o}}^{-1}\mathbf{c}_{\text{st}}(\theta,\omega)\right)} \tag{12}$$

that we shall use to evaluate performance as a function of sample support. Specifically, the minimum value of (12) over Doppler frequency, excluding the clutter notch, will be determined to ascertain the worst-case performance for each scenario.

Consider a side-looking airborne radar with N = 8 antenna elements and M = 8 pulses in the CPI. The noise is complex white Gaussian and the clutter is generated by dividing the range ring in azimuth into 65 equal-sized clutter patches, with each patch i.i.d. complex Gaussian. This spatial clutter distribution is weighted by the transmit beampattern and scaled such that, following coherent integration (pulse compression, beamforming, and Doppler processing) without clutter cancellation, the average clutter-to-noise ratio (CNR) is 50 dB. To represent the continuous environment, the received signal in (1) along with the matched filters to be applied in (2) are over-sampled by a factor of 5 relative to the nominal 3-dB range resolution. After the pulse compression stage of (2), each channel is decimated in range by 5 so that the primary training data snapshots are independent.

All SCM estimates are diagonally loaded with the noise power to provide full rank. The primary data excludes the CUT and 1 guard cell on either side. While the same is not needed for the secondary data since the secondary matched filters smear the response in range, nonetheless we shall exclude these 3 range cells for the secondary data so that the results are more convenient to illustrate in terms of the number of snapshots in the SCM. For each scenario, 50 independent Monte Carlo trials are performed.

Figure 2 shows the SINR metric from (10) for each of the nine training data combinations from Table 1 under the condition of homogeneous clutter and a range swath for training data that covers 2NM range cells. Note that this

interval means that case 'P, S1' from Table 1 has $2 \times 2NM$ training data samples and so on up to $5 \times 2NM$ samples for the 'P, S1-S4' case.

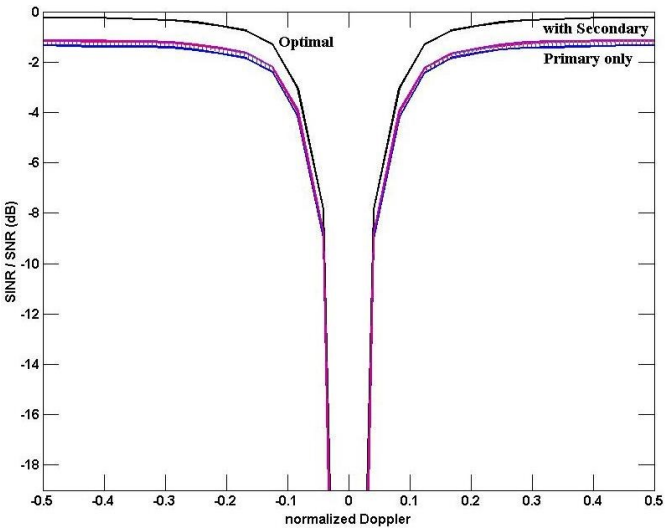

Fig. 2. SNR-normalized SINR for homogeneous clutter

The case of primary only ('P') in Fig. 2 is only marginally improved upon by using secondary data. However, examining the worst-case convergence relative to swath width in Fig. 3, it is observed that the secondary data does provide a significant convergence advantage. Also note that a "diminishing return" condition occurs as more secondary channels are included which arises from the lack of statistical independence of the secondary snapshots with respect to the primary (or each other).

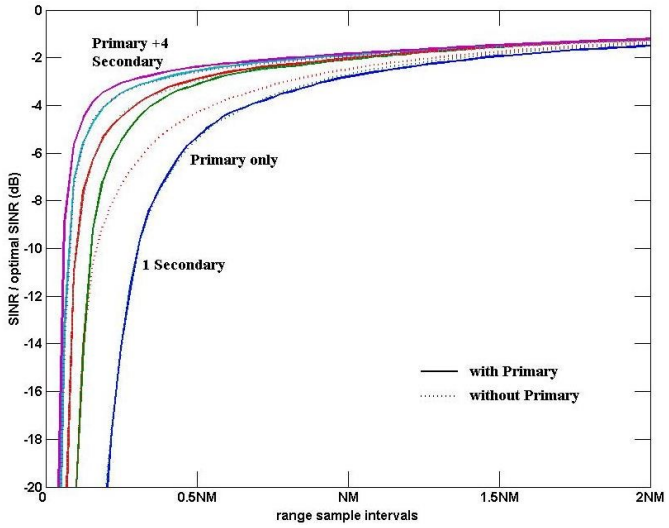

Fig. 3. Worst-case $SINR_o$-normalized SINR for homogeneous clutter

Non-homogeneous clutter is modeled where the amplitude of each clutter patch is modulated over range based on a random uniform distribution on [0, +30] dB, the patches are modulated across azimuth using a randomly parameterized sinusoidal model, and internal clutter motion uniformly distributed on ±2% of normalized Doppler is induced. The SINR metric from (10) is shown in Fig. 4 where it is observed that the clutter notch has widened but, as with Fig. 2, the impact of secondary data is again minimal. However, when the worst-case convergence performance is considered (see Fig. 5) the separation between primary-only and the use of secondary data is markedly increased compared to the previous homogeneous clutter scenario, largely due to degredation in convergence for the primary-only case.

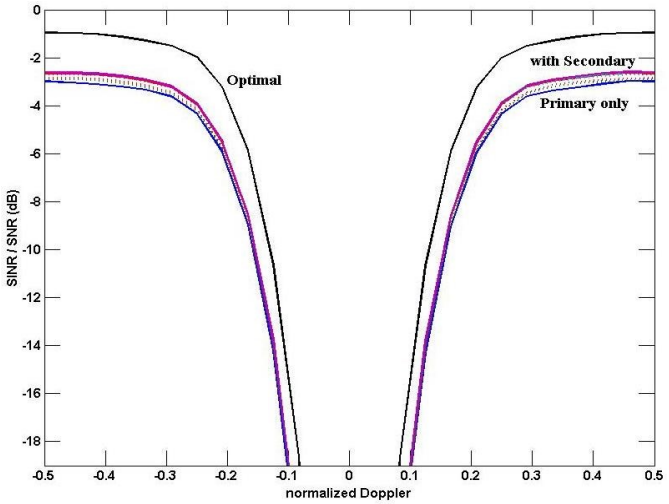

Fig. 4. SNR-normalized SINR for non-homogeneous clutter

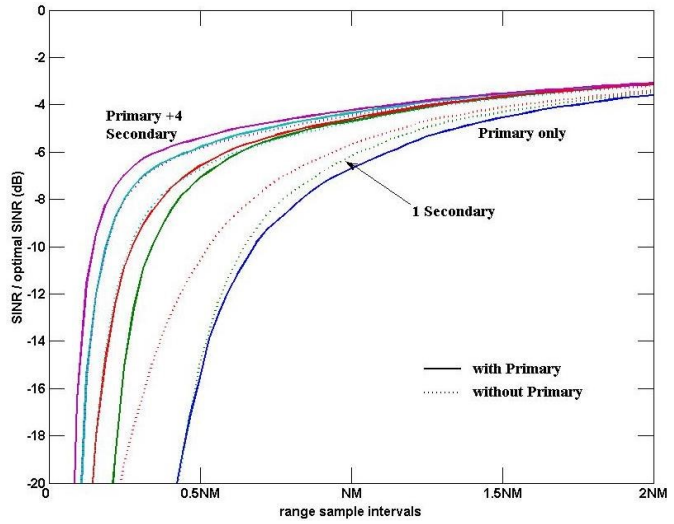

Fig. 5. Worst-case $SINR_o$-normalized SINR for non-homogeneous clutter

Severe degradation is observed when a large clutter discrete (40 dB > average clutter power) is present in the CUT in the direction of the first spatial sidelobe as this form of non-homogeneity represents a significant non-stationarity. As shown in Fig. 6, the primary-only SINR suffers roughly 2 dB loss across Doppler outside of the clutter notch. Furthermore, in terms of worst-case convergence across Doppler (Fig. 7), the primary-only case is now very poor because the discrete scatterer snapshot is absent from the training data. In contrast, the secondary data cases exhibit far greater robustness due to

the smearing effect of the secondary filters so that the clutter discrete response is present in the secondary training data.

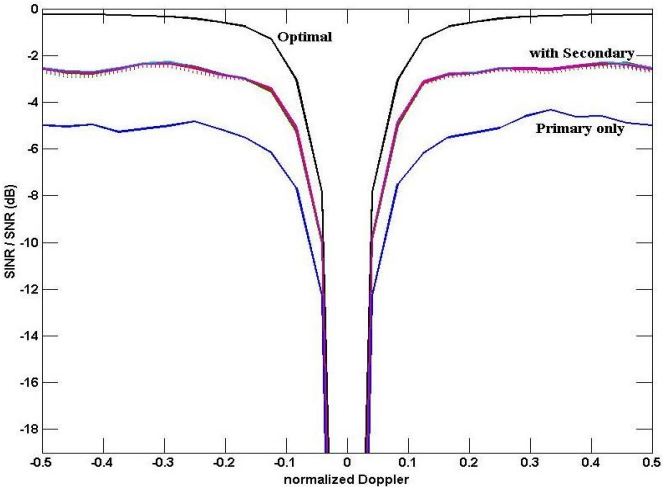

Fig. 6. SNR-normalized SINR for clutter discrete in CUT

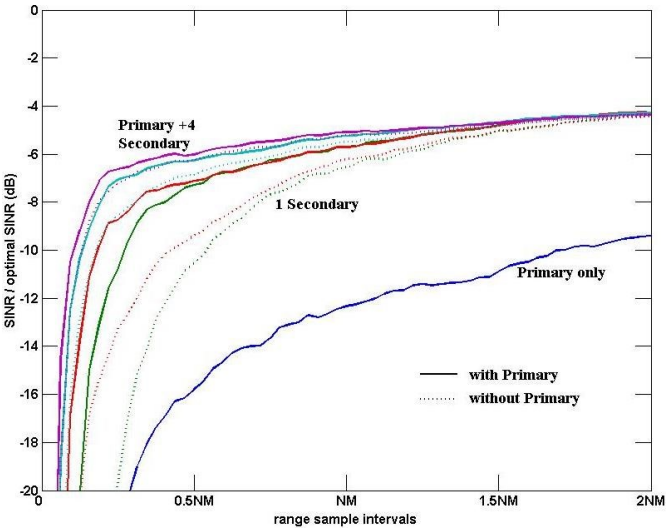

Fig. 7. Worst-case $SINR_o$-normalized SINR for clutter discrete in CUT

Finally, consider the impact of a target of interest in the training data which is known to cause self-cancellation for STAP. Here the target has an SNR of 30 dB, a normalized Doppler = 0.5, and resides in the 1st training data snapshot. Being a target of interest means that it lies in the direction of the spatial mainbeam. It is observed in Fig. 8 that both the primary-only and secondary SINR results are degraded at Dopplers near that of the contaminating target. The worst-case convergence performance (Fig. 9) is likewise degraded relative to the homogeneous baseline case from Fig. 3, though the secondary data still provides the benefit of faster convergence.

As with traditional STAP there would clearly still be a benefit from excising contaminating targets from the μ-STAP training data (e.g. [5,6]) as well. The difference here is that some form of CLEAN-type approach [15,16] may be needed to prevent smearing the target(s) during the secondary pulse compression filtering in (2). That said, observing from Fig. 9 that the cases not using the primary training data (dashed traces) provide somewhat faster convergence than their counterparts that do employ the primary training data (solid traces), it can be inferred that the unfocused response of the contaminating targets is less deleterious than a focused response. This observation therefore leads to the question of what makes for good secondary filters, a topic that is still being investigated.

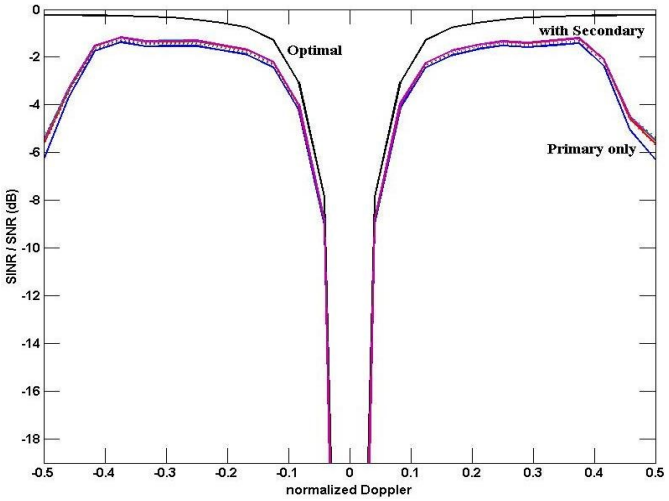

Fig. 8. SNR-normalized SINR for target in training data

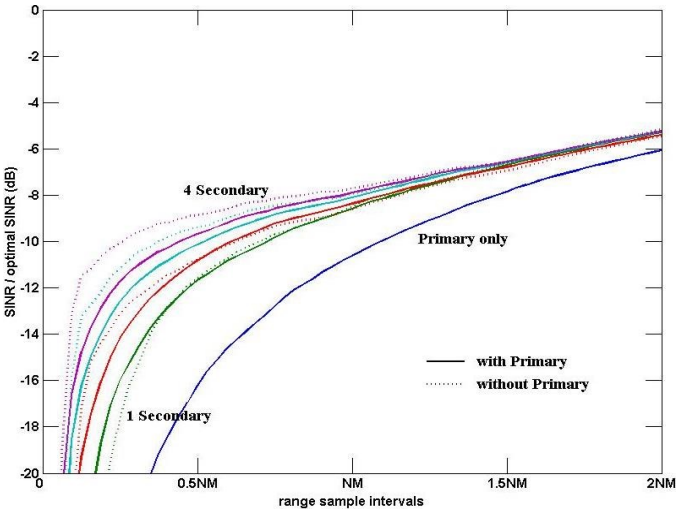

Fig. 9. Worst-case $SINR_o$-normalized SINR for target in training data

CONCLUSIONS

For the SIMO instantiation the Multi-Waveform STAP (or μ-STAP) algorithm employs multiple different pulse compression filters to produce additional training data channels for sample covariance matrix estimation. It has been found via SINR analysis that these secondary training data channels, while clearly not providing independent snapshots, still yield a significant benefit in terms of rate of convergence and robustness to some forms of non-homogeneity. The unfocused response of these secondary filters is in some ways

similar to data de-emphasis techniques as well as multi-resolution methods.

ACKNOWLEDGEMENTS

The authors would like to thank Dr. Giuseppe "Joe" Fabrizio of DSTO in Australia and Prof. James Stiles of the University of Kansas for their insights into the relationship of μ-STAP to data de-emphasis methods and multi-resolution methods, respectively.

REFERENCES

[1] S.D. Blunt, J. Jakabosky, J. Metcalf, J. Stiles, and B. Himed, "Multi-waveform STAP," *IEEE Radar Conf.*, Ottawa, Canada, 29 Apr. – 3 May 2013.

[2] J. Ward, "Space-time adaptive processing for airborne radar," *Lincoln Lab Tech. Report*, TR-1015, Dec. 1994.

[3] K. Gerlach, "Outlier resistance adaptive matched filtering," *IEEE Trans. AES*, pp. 885-901, July 2002.

[4] W.L. Melvin, "Space-time adaptive radar performance in heterogeneous clutter," *IEEE Trans. AES*, pp. 621-633, Apr. 2000.

[5] M. Rangaswamy, P. Chen, J.H. Michels, and B. Himed, "A comparison of two non-homogeneity detection methods for space-time adaptive processing," *IEEE SAM Workshop*, pp. 355-359, Aug. 2002.

[6] S.D. Blunt and K. Gerlach, "Efficient robust AMF using the FRACTA algorithm," *IEEE Trans. AES*, pp. 537-548, Apr. 2005.

[7] D.J. Rabideau and A.O. Steinhardt, "Improved adaptive clutter cancellation through data-adaptive training," *IEEE Trans. AES*, vol. 35, no. 3, pp. 879-891, July 1999.

[8] G.A. Fabrizio and M.D. Turley, "An advanced STAP implementation for surveillance radar systems," *IEEE Statistical Signal Processing Workshop*, pp. 134-137, Orchid Country Club, Singapore, 6-8 Aug. 2001.

[9] J.S. Bergin, C.M. Teixeira, and P.M. Techau, "Multi-resolution signal processing techniques for airborne radar," *IEEE Radar Conf.*, pp. 277-282, Philadelphia, PA, 26-29 Apr. 2004.

[10] G.A. Akers and J.M. Stiles, "An approach to ground moving target indication (GMTI) using multiple resolutions of the clutter covariance matrix," *IEEE Radar Conf.*, Pasadena, CA, 4-8 May 2009.

[11] J. Jakabosky, S.D. Blunt, M.R. Cook, J. Stiles, and S.A. Seguin, "Transmitter-in-the-loop optimization of physical radar emissions," *IEEE Radar Conf.*, pp. 874-879, May 2012.

[12] S.D. Blunt, M. Cook, J. Jakabosky, J. de Graaf, and E. Perrins, "Polyphase-coded FM (PCFM) radar waveforms, part I: implementation," to appear in *IEEE Trans. AES.*

[13] S.D. Blunt, J. Jakabosky, M. Cook, J. Stiles, S. Seguin, and E.L. Mokole, "Polyphase-coded FM (PCFM) radar waveforms, part II: optimization," to appear in *IEEE Trans. AES.*

[14] W. Melvin, "A STAP overview," *IEEE A&E Systems Magazine*, vol. 19, no. 1, pp. 19-35, Jan. 2004.

[15] Y.I. Abramovich, "Compensation methods for the resolution of wideband signals," *Radio Eng. Elect. Phys.*, vol. 23, no. 1, pp. 54-59, Jan. 1978.

[16] H. Deng, "Effective CLEAN algorithms for performance-enhanced detection of binary coding radar signals," *IEEE Trans. Signal Processing*, vol. 52, no. 1, pp. 72-78, Jan. 2004.